Contrast-enhanced Multispectral Optoacoustic Tomography for Functional Assessment of the Gastrointestinal Tract

Ferdinand Knieling (ferdinand.knieling@uk-erlangen.de)
University of Erlangen-Nuremberg https://orcid.org/0000-0002-3535-2626

Lars-Philip Paulus
University Hospital Erlangen

Adrian Buehler
University of Erlangen-Nuremberg

Alexandra Wagner
University Hospital Erlangen

Roman Raming
University Hospital Erlangen

Jörg Jüngert
Department of Pediatrics and Adolescent Medicine, Friedrich-Alexander-University of Erlangen-Nuremberg

David Simon
University of Erlangen-Nuremberg https://orcid.org/0000-0001-8310-7820

Koray Tascilar
Department of Internal Medicine 3, Friedrich-Alexander University (FAU) Erlangen- Nuremberg and Universitätsklinikum Erlangen https://orcid.org/0000-0002-8109-826X

Alexander Schnell
University Hospital Erlangen

Ulrich Rother
Department of Vascular Surgery, University Hospital Erlangen, Friedrich-Alexander-Universität Erlangen-Nürnberg (FAU)

Werner Lang
Department of Vascular Surgery, University Hospital Erlangen, Friedrich-Alexander-Universität Erlangen-Nürnberg (FAU) https://orcid.org/0000-0003-4114-7589

André Hörning
University Hospital Erlangen

Georg Schett
FAU Erlangen-Nuremberg https://orcid.org/0000-0001-8740-9615

Markus Neurath

FAU-Uniklinikum Erlangen https://orcid.org/0000-0003-4344-1474
Maximilian Waldner
University of Erlangen-Nuremberg
Regina Trollmann
Friedrich-Alexander Universität Erlangen-Nürnberg https://orcid.org/0000-0001-6031-8537
Joachim Wölfle
Friedrich-Alexander-Universitaet Erlangen-Nuermberg
Sarah Bohndiek
University of Cambridge https://orcid.org/0000-0003-0371-8635
Adrian Regensburger
University Hospital Erlangen, Friedrich-Alexander-Universität Erlangen-Nürnberg (FAU)
https://orcid.org/0000-0001-8244-1261
Markus Eckstein
University Hospital Erlangen https://orcid.org/0000-0001-5418-3349

Article

Keywords: Optoacoustics, Photoacoustics, Multispectral Optoacoustic Tomography, Intestine, Indocyanine green

Posted Date: December 20th, 2022

DOI: https://doi.org/10.21203/rs.3.rs-2380754/v1

Abstract

Real-time imaging and functional assessment of the intestinal tract and its transit poses a significant challenge to traditional clinical diagnostic methods. Multispectral optoacoustic tomography (MSOT), a molecular-sensitive imaging technology, offers the potential to visualize endogenous and exogenous chromophores in tissue. Herein we present a novel approach using the orally administered clinical-approved fluorescent dye indocyanine green (ICG) for bed-side, non-ionizing evaluation of gastrointestinal passage. We were able to show the detectability and stability of ICG in phantom experiments. Furthermore, ten healthy subjects underwent MSOT imaging at multiple timepoints over eight hours after ingestion of a standardized meal with and without ICG. ICG signals could be visualized and quantified in different intestinal segments, while its excretion was confirmed by fluorescent imaging of stool samples. These findings indicate that contrast-enhanced MSOT (CE-MSOT) provides a translatable real-time imaging approach for functional assessment of the gastrointestinal tract.

Introduction

Despite the availability of sophisticated cross-sectional imaging techniques, anatomical and functional assessment of the gut – especially in children – is still frequently performed using X-ray fluoroscopy [1]. Such procedures require skilled interpretation, use ionizing radiation, and may have limited diagnostic information [2].

Alternatively, ultrasound imaging techniques offer high-resolution, real-time radiation-free imaging capabilities [3, 4]. Multispectral optoacoustic tomography (MSOT) combined with ultrasound can be seen as a further development in this field, which, in addition to anatomical B-mode information, also enables molecular imaging of tissues [5]. MSOT relies on absorption of laser light excitation in the near-infrared window to induce a thermoelastic response, resulting in detectable ultrasound waves [6], which allows the visualization and quantification of different endogenous chromophores like hemoglobin, lipids, and collagens [6–9]. Label-free clinical MSOT has already demonstrated feasibility for non-invasive assessment of hemoglobin signals as surrogate markers for intestinal inflammatory activity [10, 11].

To increase the specificity for detection, externally applied contrast agents with distinct optoacoustic spectra [12, 13] can be used for precise optoacoustic visualization [14–16]. While contrast-enhanced imaging typically requires intravenous application and in optics, often near surface detection, [17, 18], MSOT goes beyond these limitations and enables clinically relevant transabdominal deep tissue penetration [19–21].

We hypothesized that oral administration of indocyanine green (ICG), a clinical approved dye, might enable the visualization of gastrointestinal passage in a non-invasive radiation-free manner to close the gap in the current standard-of-care. To test this hypothesis, we performed phantom experiments and a clinical trial for immediate translation of this approach for clinical applications.

Materials And Methods

Phantom experiments

For phantom experiments, custom-made molds were designed using Autodesk Fusion 360 (V2.0.14567, Autodesk GmbH, München, Germany) and printed with a 3D printer (Form 2, Formlabs. Inc, Somerville, MA, USA) using White Resin V4 (Formlabs. Inc, Somerville, MA, USA). Two molds were filled with 2% Agarose (Biozym LE Agarose, Biozym Scientific GmbH, Hessisch Oldendorf, Germany) dissolved in distillated water to cast an agarose phantom with the body dimension of 96 * 46 * 40 mm and a matching cover of 96 * 46 * 10 mm. Inside the body part a 76 * 26 * 20 mm recess was used to be filled with different contents and sealed with the agarose cover. For the experiments, a standardized meal [22] (approximately 450 mL, **Supplementary Table 1**) was blended and divided into 112.5 mL portions for each phantom setup. ICG (Verdye 5mg/mL, Diagnostic Green, Aschheim-Dornach, Germany) was reconstituted according to the manufacturers recommendations and different amounts of the solution were added to achieve the final concentrations in the blended meal samples. To test the stability of ICG signals at varying pH levels, one portion of the blended meal was acidified to a pH of 2.5 using 1.2 mL of 32% HCl before ICG was added. Another portion was similarly treated and adjusted to a pH of 7 using 1.6 mL of 32% NaOH. This should simulate the change of pH during the gastrointestinal transit from the stomach to the duodenum and small intestine. Furthermore, another portion was acidified with access 32% HCl to reach a pH below 1 (**Supplementary Table 2**).

For all experiments the MSOT imaging probe (MSOT Acuity CE, iThera Medical, München, Germany) was mounted in a laboratory bracket and coupled to the agarose phantom using transparent ultrasound gel (Aquasonic Clear, MDSS GmbH, Hannover, Germany).

Design and flow of the study

The prospective single-center investigator initiated trial (IIT) was conducted from November 2021 to January 2022 at the Department of Pediatric and Adolescent Medicine at the University Hospital Erlangen. Approval from the local ethics committee was granted (346_21B) and the clinical trial was registered (clinicaltrials.gov identifier NCT05160077) before study initiation. The Declaration of Helsinki was respected and all subjects gave their written informed consent.

This study included n = 10 healthy subjects aged over 18 years. Exclusion criteria were pregnancy, nursing mothers, tattoo in the field of investigation, subcutaneous fat tissue over 3 cm, preexisting chronic or acute diseases of the gastrointestinal tract or symptoms suggestive of such a disease, a diseases requiring acute treatment and the lack of written consent. Futhermore, any known hypersensitivity to ICG, sodium iodide or iodine, hyperthyroidism, focal or diffuse thyroid autonomy, treatment with radioactive iodine for the diagnostic examination of thyroid function within two weeks before or after the study and restricted renal function. The following co-medications also lead to an exclusion: Beta-blockers, anticonvulsants, cyclopropane, bisulphite compounds, haloperidol, heroin, meperidine, metamizole,

methadone, morphine, nitrofurantoin, opium alkaloids, phenobarbital, phenylbutazone, probenecid, rifamycin, any injection containing sodium bisulphite.

After inclusions, subjects were examined on two seperate days, one with standardized meals, the other with standardized meals and oral ICG intake. For every day, two subjects were fasting since the evening before and started the examinations on the next day at 8:00 or 8:30am, respectively. All subjects were imaged at n = 8 timepoints with an interval of 60 minutes inbetween. Before each imaging timepoint, subjects were advised to drink 150 mL of water, which reflects the recommended daily water amout of 1.500–2000 mL. 30 minutes after the first and fourth imaging timepoint a standardized meal (500 kcal for women and 650 kcal for men − 55% carbohydrates, 29% fat, and 16% proteins [22]) was given. On the second day 50mg of ICG (Verdye 5mg/ml, Diagnostic Green GmbH, Aschheim-Dornach, Germany) dissolved in 150mL water) was orally administered in one go with the first meal. Anatomical locations for imaging were as follows: gastric antrum, terminal ileum, transverse colon, sigmoid colon. Two MSOT scans per location were performed at each timepoint.

MSOT Device

The identical CE-certified MSOT system (Acuity ECHO CE, iThera medical GmbH, Munich, Germany) was used for experimental and clinical studies. This system enables hybrid B-mode and optoacoustic imaging [23, 24]. All subjects were investigated with a handheld 2D detector and coupling was achieved by transparent ultrasound gel (Aquasonic Clear, MDSS GmbH, Hannover, Germany). All attending persons wore laser safety goggles during imaging. All anatomical regions were identified by B-mode imaging and optoacoustic signals were acquired at 700, 730, 760, 800, 850, and 900 nm.

Fluorescence imaging

On the next day after ICG ingestion, n = 3 consecutive stool samples were collected from n = 5 subjects. The fluorescent properties of these samples were examined using an *in vivo* imaging system (IVIS® Spectrum, PerlkinElmer Inc., Waltham, Massachusetts, United Staates) using excitation wavelengths of 570, 605, 640, 675, 710, 745 nm and emission wavelengths of 760, 780, 800, 820, 840 nm. To spectrally unmix for ICG signals in the stool samples, the factory presets for ICG fluorescence and tissue autofluorescence signals were used.

Data analysis of MSOT scans

For analysis of phantom experiments, regions of interest (ROI) were drawn directly below the upper border of the recess in the agarose phantom to include the ICG signal using software supplied by the vendor (ViewMSOT version ??; iThera Medical GmbH). For all scans of the clinical study, ROIs resembling the upper bowel wall were drawn directly after image acquisition guided by the B-mode image. The data were then transferred and processed with iLabs software (V 1.3.16, iThera medical GmbH, Munich, Germany) as follows: ROIs were checked by a second reader. After final placement, ROIs of the clinical study were automatically enlarged by 2mm in depth using a custom-written script to include the bowel lumen/stool as the potential area of ICG signals. This approach was used to ensure similar analysis of scans with and

without visible ICG singals. Within each ROI the mean of the highest 10% of pixels were used for batch mode quantification of single wavelengths and unmixed ICG signal levels. Spectral unmixing of ICG was performed using four different presets (A-D), each of which used a different reference spectrum for ICG in plasma, to account for the concentration-dependent change in the ICG spectrum (reference spectra taken at 6.5, 65, 650, and 1290µM). Spectral unmixing was applied to MSOT data acquired using the following wavelengths: 700, 730, 760, 800, and 850nm.

Statistics

Demographic data of all subjects is presented as numbers and percentages or mean and standard deviation. For MSOT signal analyses, data was tested for normal distribution by Shapiro Wilk test. The MSOT spectra in phantom experiments were normalized to the value at 760 nm, since at this wavelength the molecular extinction coefficient is stable between spectra. For clinical data, absolute values were used. For each imaging timepoint during the meal + ICG experiment, the value was tested against the mean of day meal without ICG using Kruskal-Wallis test with Dunn´s correction. *P*-values < 0.05 indicate statistical significance. All statistical analyses were calculated by GraphPad Prism (Version 9, GraphPad Software Inc., La Jolla, USA).

Results

ICG imaging in phantom

For all experiments, a handheld clinically-certified MSOT was used for ICG imaging (Fig. 1a). To differentiate ICG from background chromophores such as hemoglobin, spectral unmixing was applied using the unique absorption spectra of the molecules of interest. The absorption spectra of ICG are known to change slightly in a dose-dependent manner, but all peak at around 800nm (Fig. 1b). In phantom experiments, blended meals with and without ICG at five different concentrations (1.06–212µM) were examined for their respective optoacoustic spectra (Fig. 1c + d). ICG concentrations ranging from 10.6–212µM confirmed a signal maximum at 800nm in accordance with the molecular extinction coefficient derived from literature (Fig. 1b + d). In anticipation of the clinical study, in which all subjects had a standardized meal with an ICG concentration of about 106 µM (50 mg ICG in 150 mL of water with a meal of approximately 450 mL), we wanted to investigate the limit of detection for ICG in the phantom setting. Assuming the concentration decreases due to large distribution volume in gastrointestinal tract, ICG concentrations between 0 and 212 µM were tested. As demonstrated, all concentrations down to 0.106µM were detected by MSOT while the negative control did not show any evidence of ICG (Fig. 1e). To mimic gastric passage and its acid condition, we confirmed that changing of pH leveles had no relevant influence on the dection of ICG by MSOT (Fig. 1e). With the clinical MSOT system, four ICG spectral unmixing settings were available for data analysis derived from the concentration-dependent molecular extinction spectra of ICG in plasma from Landsman et al [13]. The use of preset A (using the spectrum derived from an ICG concentration of 6.5 µM) showed the best discrimination between different samples (Fig. 1f).

Clinical proof-of-concept trial

n = 10 healthy subjects (n = 6 female) were investigated within the clinical trial. The subjects had a mean ± SD age of 22.5 ± 1.2 years, height of 174.7 ± 9.1 cm, weight of 66.5 ± 7.8 kg and BMI 21.7 ± 1.1 kg/m^2. Transabdominal MSOT imaging of four anatomical locations was performed consecutively at each of eight imaging timepoints every 60 minutes on two days with an interval of at least 48 hours inbetween (Fig. 2a + b). All subjects had two standardized meals and on the second imaging day with an additional oral intake of 50mg ICG. MSOT imaging was guided by hybrid B-mode ultrasound to identify the intestinal segments. After image acquisition, semi-automated ROI extension and subsequent batch mode analyses of MSOT ICG signals with different ICG spectral unmixing presets was performed (Fig. 2c). The presented analyses were computed with an ICG unmixing preset A (derived from ICG concentration of 6.5µM in plasma). As described above, this showed the most distinguishable results in phantom experiments and might reflect the *in vivo* situation best with decreased ICG concentrations in the downstream intestinal segments. All analyses were similiarly re-performed with the other spectral unmixing presets, indicating similar results (see Supplementary Fig. 1–3).

In vivo contrast-enhanced MSOT in humans

At the beginning of the clinical study, no relevant ICG signals were seen throughout all observed intestinal segments. In the gastric antrum, ICG signals were increased after 1.5h (25.4 ± 3.8 x10^{-5} vs. 30.5 ± 2.7x10^{-5} a.u., P = 0.0010). At this timepoint, first signal increases were also detectable in the more distal terminal ileum (Fig. 3a, **Supplementary Video 1**). Herein, unmixed ICG signals were elevated over the time range from 2.5 to 24h with a maximum after 5.5h (34.8 ± 18.3 x10^{-5} vs. 113.5 ± 81.1x10^{-5} a.u., P< 0.0001). However, no significant differences in MSOT ICG signal intensity was found in the transversal colon. In the more distal locations, such as the sigmoid colon, there was an enrichment of the signal after 24 hours (29.4 ± 6.4x10^{-5} vs. 77.1 ± 44.7x10^{-5} a.u., P = 0.0008) (Fig. 3b, **Supplementary Video 2**).

Proof of successful gastrointestinal passage

As MSOT ICG signal increase in the colon was only seen 24 hours after ICG intake, we wanted to confirm a successful passage of the compound through the gastrointestinal tract without systemic uptake or intestinal degradation (Fig. 4a). Therefore, fluorescent imaging was performed on three subsequent stool samples from n = 5 subjects and confirmed its presence in the faeces of the participants (Fig. 4b). The three stool samples were collected 16.7 ± 17.25h, 30.6 ± 23.59h and 42.75 ± 30.55h hours after ICG ingestion. 3 out of 5 samples from the first timepoint and all further sample were positive for ICG fluorescence. To further confirm the presence of ICG, optoacoustic spectra were compared at the imaging timepoints with the greatest ICG signal intensities. The optoacoustic spectra 5.5 hours after ICG intake the terminal ileum and 24 hours after ICG intake in the sigmoid colon were found to be similar to the one derived from ICG phantom experiments as compared to standardized meal without ICG (Fig. 4c).

Discussion

In this translational study we have demonstrated the technical and clinical feasibility of CE-MSOT for functional imaging of the intestine. While phantom experiments showed that ICG detection is possible over a wide range of concentrations and pH conditions, subsequent human imaging confirmed feasibility for *in vivo* imaging of the human intestine. Furthermore, fluorescent ICG signals were also detectable in stool samples after application of the dye.

ICG, a dye already approved for intravenous use in children, adolescents and adults, was already shown for broad applications in preclinical [25–27] and clinical studies [28, 29]. Similarly to the current study, Morscher et al demonstrated its oral use for imaging gastric emptying in mice [30]. Beyond these animal experiments, we demonstrated the feasability of this drug/device combination for hand-held, bed-side imaging of the intestine with broad clinical implications. CE-MSOT could provide a bed-side assessment of the gastrointestinal passage and prolonged transit times in patients chronic constipation without harmful ionizing or radioactice radiation of diagnostic standards like radio opaque marker testing [31, 32] and szintigraphy [33]. Furthermore, very young patients suspected of intestinal malformation, obstruction, functional bowel disorders or fistulae [34, 35] and chronic ill patients with strictures caused by inflammatory diseases [36] could benefit from such a non-invasive, radiation-free molecular-sensitive imaging approach, which could complement established magnetic resonance imaging or computed tomography protocols [37].

In contrast to other studies, we used a clinical-grade ICG compound and avoided the generation of any encapsuled formulations in order to potentially reduce degradation of the contrast agent [38]. Our phantoms experiments prove that an acid environment does not affect the optoacoustic properties of ICG and its stability within the gut was proven by its detection in stool samples.

In the future, targeting of the imaging compound may enable targeted imaging in the human intestine to directly flag inflammatory or malignant processes [39]. In comparison to molecular endoscopy [17, 40], which uses similar principles, targeted CE-MSOT with oral administration may avoid any invasive imaging procedures. However, prior targeted optoacoustic imaging studies using intravenous application of either cetuximab-800CW [41] or panitumumab-IRDye800CW [42] for detection of cancer metastasis showed heterogeneous results. The amounts of imaging agents given via systematic circulation might not have been sufficient to produce enough signal in comparison to background noise. This problem was not present in our study, wherein we used 50mg of ICG, which is significantly below the maximum recommend daily intravenous dose of 1.25mg/kg per bodyweight. Thus, a systematic uptake of ICG in inflamed intestinal segments should not represent a relevant problem. In addition, oral as opposed to intravenous administration allowed us to circumvent the problem of possible misinterpretation of strong interfering hemoglobin signals in vessels. However, the influence of light absorption and optoacoustic signals arising from intestinal contents is unclear and should be investigated in further studies.

This study has several limitations. The reliable identification of anatomical structures is significantly more difficult with optoacoustic imaging, so a hybrid approach with B-mode imaging was required to

guide the examiner [23, 24]. Imaging of signals in the gastric and transversal colon regions was not equal to the terminal ileum and sigmoid colon. In the stomach, no ICG enhancement was detectable after ICG ingestion even though an increased gastric filling was visible in the B-mode image on timepoints directly after the meals. One reason might be the quick transit of liquids through gastric canals along the small curvature without proper mixing with solid food components [43, 44]. For the transverse colon chyme retention time is most likely too short that the ICG could be imaged. Also the distribution and dilution/concentration of ICG in the intestine at different anatomical locations is largely unknown. In this regard, we have shown that ICG was detectable from in a concentration of of 200–0.1% ofthe original meal with ICG (106 µM). Visually ICG signals within the intestine had the greatest similarity with signals from the phantom at 1.06 µM, indicating a rather low concentration in the gut.

In summary, the present translational study demonstrated the feasibility of MSOT for detection of an oral applied clinical approved dye inside the gastrointestinal tract. In contrast to other modalities, CE-MSOT does not require any radiation and enables deep tissue detection. This suggest an immediate clinical translation in order to minimize the number of more invasive and burdensome examinations, while opening the window for novel molecular imaging of gastrointestinal pathologies of functional and structural nature.

Declarations

Acknowledgement

We thank Yi Qiu (iThera Medical GmbH, Munich, Germany) for iLabs software support.

Funding

The Interdisciplinary Center for Clinical Research (IZKF) at the University Hospital of the Friedrich-Alexander-Universität (FAU) funded this project (J89 and CSP program to APR and MD-thesis scholarship to LPP). The present work was performed in fulfillment of the requirements for obtaining the degree “Dr. med.” for LPP at the Friedrich-Alexander-Universität Erlangen-Nürnberg (FAU). SEB acknowledges support from CRUK (C9545/A29580).

Conflicts of interest

MJW, FK, and APR are shared patent holders together with iThera Medical on an optoacoustic imaging system/software described in the study.

Author contribution

LPP, APR, and FK conceived the idea of the study. FK was the principle investigator. LPP, RR, APR and FK performed preclinical and clinical imaging (MSOT and ultrasound). SEB helped with phantom imaging design und spectral analysis. LPP, KT, DS, APR, and FK performed (statistical) data analysis. LPP, ALW, APB, RR, JJ, DS, KT, AS, UR, ME, WL, AH, GS, MFN, JW, MJW, FK, and APR interpreted the data. LPP, APR,

and FK wrote the first draft of the manuscript. All other authores revised it critically for important intellectual content and approved the final version of the manuscript.

Data availability statement

Data is available from the corresponding author on resonable request.

References

1. Kurugoglu, S., et al., *Enteroclysis in older children and teenagers*. Pediatr Radiol, 2007. **37**(5): p. 457–66.
2. Arthurs, O.J., et al., *Interactive neonatal gastrointestinal magnetic resonance imaging using fruit juice as an oral contrast media*. BMC Med Imaging, 2014. **14**: p. 33.
3. Sanchez, T.R., B. Doskocil, and R. Stein-Wexler, *Nonsurgical management of childhood intussusception: retrospective comparison between sonographic and fluoroscopic guidance*. J Ultrasound Med, 2015. **34**(1): p. 59–63.
4. Anupindi, S.A., et al., *Pediatric inflammatory bowel disease: imaging issues with targeted solutions*. Abdom Imaging, 2015. **40**(5): p. 975–92.
5. Regensburger, A.P., et al., *Shedding light on pediatric diseases: multispectral optoacoustic tomography at the doorway to clinical applications*. Mol Cell Pediatr, 2020. **7**(1): p. 3.
6. Ntziachristos, V. and D. Razansky, *Molecular imaging by means of multispectral optoacoustic tomography (MSOT)*. Chem Rev, 2010. **110**(5): p. 2783–94.
7. Tzoumas, S., et al., *Unmixing Molecular Agents From Absorbing Tissue in Multispectral Optoacoustic Tomography*. IEEE Trans Med Imaging, 2014. **33**(1): p. 48–60.
8. Regensburger, A.P., et al., *Detection of collagens by multispectral optoacoustic tomography as an imaging biomarker for Duchenne muscular dystrophy*. Nat Med, 2019. **25**(12): p. 1905–1915.
9. Cao, Q., et al., *Multispectral imaging in the extended near-infrared window based on endogenous chromophores*. J Biomed Opt, 2013. **18**(10): p. 101318.
10. Waldner, M.J., et al., *Multispectral Optoacoustic Tomography in Crohn's Disease: Noninvasive Imaging of Disease Activity*. Gastroenterology, 2016. **151**(2): p. 238–40.
11. Knieling, F., et al., *Multispectral Optoacoustic Tomography for Assessment of Crohn's Disease Activity*. N Engl J Med, 2017. **376**(13): p. 1292–1294.
12. Fuenzalida Werner, J.P., et al., *Challenging a Preconception: Optoacoustic Spectrum Differs from the Optical Absorption Spectrum of Proteins and Dyes for Molecular Imaging*. Anal Chem, 2020. **92**(15): p. 10717–10724.
13. Landsman, M.L., et al., *Light-absorbing properties, stability, and spectral stabilization of indocyanine green*. J Appl Physiol, 1976. **40**(4): p. 575–83.
14. Buehler, A., et al., *Video rate optoacoustic tomography of mouse kidney perfusion*. Opt Lett, 2010. **35**(14): p. 2475–7.

15. Brillant, N., et al., *Dynamic and accurate assessment of acetaminophen-induced hepatotoxicity by integrated photoacoustic imaging and mechanistic biomarkers in vivo*. Toxicol Appl Pharmacol, 2017. **332**: p. 64–74.
16. Burton, N.C., et al., *Multispectral opto-acoustic tomography (MSOT) of the brain and glioblastoma characterization*. Neuroimage, 2013. **65**: p. 522–8.
17. Lee, J.H. and T.D. Wang, *Molecular endoscopy for targeted imaging in the digestive tract*. Lancet Gastroenterol Hepatol, 2016. **1**(2): p. 147–155.
18. Chen, Q.Y., et al., *Safety and Efficacy of Indocyanine Green Tracer-Guided Lymph Node Dissection During Laparoscopic Radical Gastrectomy in Patients With Gastric Cancer: A Randomized Clinical Trial*. JAMA Surg, 2020. **155**(4): p. 300–311.
19. Schellenberg, M.W. and H.K. Hunt, *Hand-held optoacoustic imaging: A review*. Photoacoustics, 2018. **11**: p. 14–27.
20. Steinberg, I., et al., *Photoacoustic clinical imaging*. Photoacoustics, 2019. **14**: p. 77–98.
21. Regensburger, A.P., et al., Optoacoustic Imaging in Inflammation. Biomedicines, 2021. **9**(5).
22. Goertz, R.S., et al., *Impact of food intake, ultrasound transducer, breathing maneuvers and body position on acoustic radiation force impulse (ARFI) elastometry of the liver*. Ultraschall Med, 2012. **33**(4): p. 380–5.
23. Mercep, E., et al., *Hybrid optoacoustic tomography and pulse-echo ultrasonography using concave arrays*. IEEE Trans Ultrason Ferroelectr Freq Control, 2015. **62**(9): p. 1651–61.
24. Mercep, E., X.L. Dean-Ben, and D. Razansky, *Combined Pulse-Echo Ultrasound and Multispectral Optoacoustic Tomography With a Multi-Segment Detector Array*. IEEE Trans Med Imaging, 2017. **36**(10): p. 2129–2137.
25. Bhatnagar, S., et al., *Oral Administration and Detection of a Near-Infrared Molecular Imaging Agent in an Orthotopic Mouse Model for Breast Cancer Screening*. Mol Pharm, 2018. **15**(5): p. 1746–1754.
26. Beringhs, A.O., et al., *Sublingual indocyanine green films for non-invasive swallowing assessment and inflammation detection through NIR/SWIR optical imaging*. Sci Rep, 2020. **10**(1): p. 14003.
27. Kim, C., et al., *Sentinel lymph nodes and lymphatic vessels: noninvasive dual-modality in vivo mapping by using indocyanine green in rats–volumetric spectroscopic photoacoustic imaging and planar fluorescence imaging*. Radiology, 2010. **255**(2): p. 442–50.
28. Stoffels, I., et al., *Metastatic status of sentinel lymph nodes in melanoma determined noninvasively with multispectral optoacoustic imaging*. Sci Transl Med, 2015. **7**(317): p. 317ra199.
29. Stoffels, I., et al., *Assessment of Nonradioactive Multispectral Optoacoustic Tomographic Imaging With Conventional Lymphoscintigraphic Imaging for Sentinel Lymph Node Biopsy in Melanoma*. JAMA Netw Open, 2019. **2**(8): p. e199020.
30. Morscher, S., et al., *Semi-quantitative Multispectral Optoacoustic Tomography (MSOT) for volumetric PK imaging of gastric emptying*. Photoacoustics, 2014. **2**(3): p. 103–10.

31. Hinton, J.M., J.E. Lennard-Jones, and A.C. Young, *A ne method for studying gut transit times using radioopaque markers*. Gut, 1969. **10**(10): p. 842–7.
32. Schindlbeck, N.E., A.G. Klauser, and S.A. Muller-Lissner, *[Measurement of colon transit time]*. Z Gastroenterol, 1990. **28**(8): p. 399–404.
33. Ziessman, H.A., *Gastrointestinal Transit Assessment: Role of Scintigraphy: Where Are We Now? Where Are We Going?* Curr Treat Options Gastroenterol, 2016. **14**(4): p. 452–460.
34. Applegate, K.E. and D.D. Maglinte, *Imaging of the bowel in children: new imaging techniques*. Pediatr Radiol, 2008. **38 Suppl 2**: p. S272-4.
35. Carroll, A.G., et al., *Comparative Effectiveness of Imaging Modalities for the Diagnosis of Intestinal Obstruction in Neonates and Infants:: A Critically Appraised Topic*. Acad Radiol, 2016. **23**(5): p. 559–68.
36. Rieder, F., et al., *European Crohn's and Colitis Organisation Topical Review on Prediction, Diagnosis and Management of Fibrostenosing Crohn's Disease*. J Crohns Colitis, 2016. **10**(8): p. 873–85.
37. Bettenworth, D. and F. Rieder, *Medical therapy of stricturing Crohn's disease: what the gut can learn from other organs - a systematic review*. Fibrogenesis Tissue Repair, 2014. **7**(1): p. 5.
38. Wood, C.A., et al., *Clinically translatable quantitative molecular photoacoustic imaging with liposome-encapsulated ICG J-aggregates*. Nat Commun, 2021. **12**(1): p. 5410.
39. Wang, R., et al., *Antibody-conjugated liposomes loaded with indocyanine green for oral targeted photoacoustic imaging-guided sonodynamic therapy of Helicobacter pylori infection*. Acta Biomater, 2022. **143**: p. 418–427.
40. Atreya, R., et al., *In vivo imaging using fluorescent antibodies to tumor necrosis factor predicts therapeutic response in Crohn's disease*. Nat Med, 2014. **20**(3): p. 313–8.
41. Vonk, J., et al., *Multispectral optoacoustic tomography for in vivo detection of lymph node metastases in oral cancer patients using an EGFR-targeted contrast agent and intrinsic tissue contrast: A proof-of-concept study*. Photoacoustics, 2022. **26**: p. 100362.
42. Nishio, N., et al., *Photoacoustic Molecular Imaging for the Identification of Lymph Node Metastasis in Head and Neck Cancer Using an Anti-EGFR Antibody-Dye Conjugate*. J Nucl Med, 2021. **62**(5): p. 648–655.
43. Grimm, M., et al., *Gastric Water Emptying under Fed State Clinical Trial Conditions Is as Fast as under Fasted Conditions*. Mol Pharm, 2017. **14**(12): p. 4262–4271.
44. Pal, A., J.G. Brasseur, and B. Abrahamsson, *A stomach road or "Magenstrasse" for gastric emptying*. J Biomech, 2007. **40**(6): p. 1202–10.

Figures

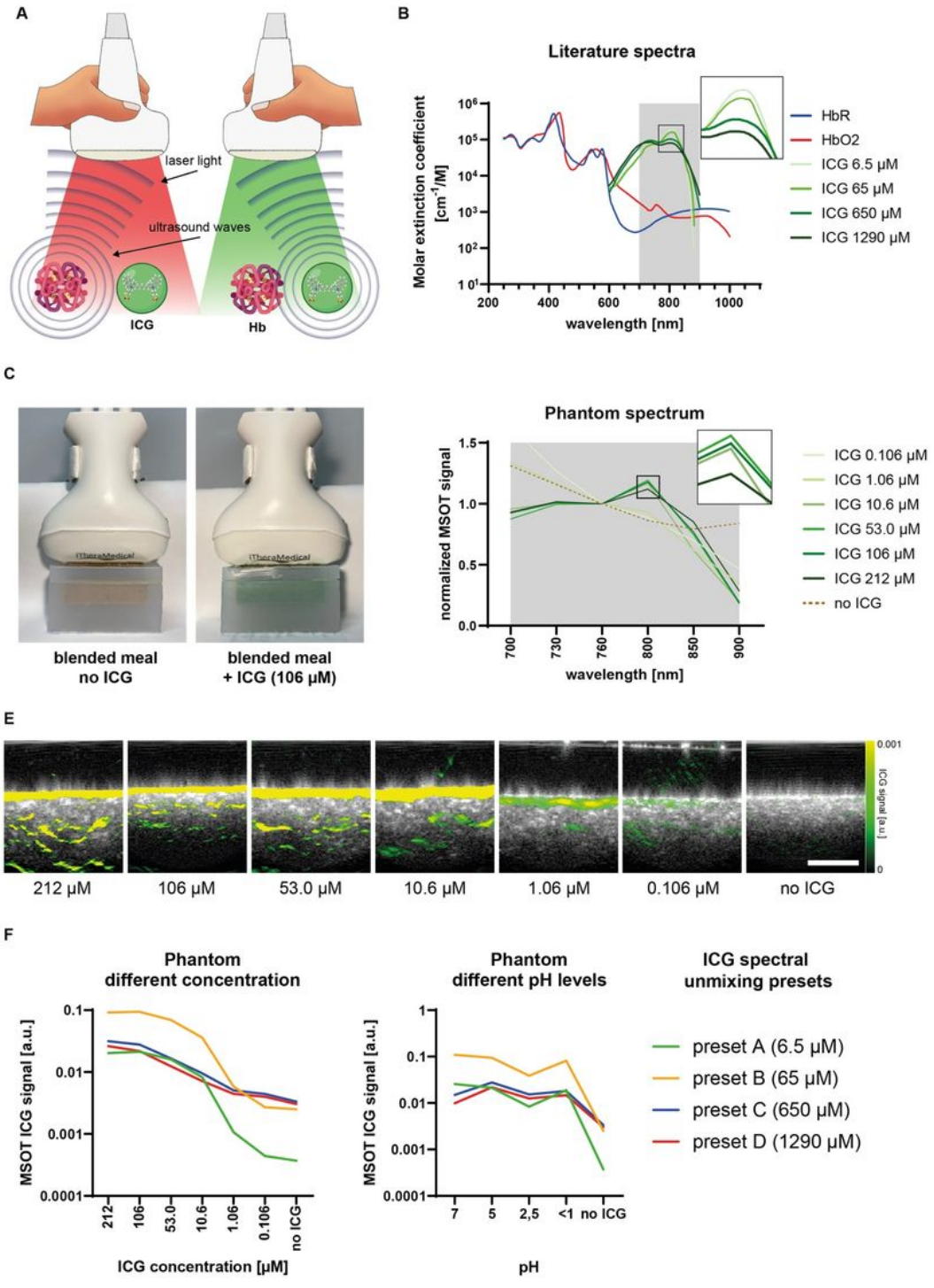

Figure 1

Multispectral optoacoustic imaging of ICG in phantoms

A: Handheld multispectral optoacoustic tomography emits laser light at different wavelengths allowing differentiation of various chromophores such as hemoglobin or indocyanine green (ICG). Hb = hemoglobin, ICG = Indocyanine green. Image created with BioRender.com.

B: Endogenous (hemoglobin) and exogenous (ICG) chromophores and their respective molecular excition coefficients in the near infrared range of light. HbR = deoxygenated hemoglobin, HbO2 = oxygenated hemoglobin, ICG = indocyanine green

C: Agarose phantoms from 3D printed molds filled with standardized blended meals with and without ICG for MSOT imaging.

D: Optoacoustic spectra derived from phantoms with blended meals with and without ICG (concentrations range between 1.06 and 212µM). Absolute values are normalized on the 760 nm signals for each dataset.

E: MSOT ICG signals detected in phantoms with blended meals with and without ICG (concentrations range between 0.106 and 212µM). White bar represents 1cm.

F: MSOT ICG signals derived from different spectal unmixing settings (present A-D) in phantoms with different ICG concentrations and pH levels.

Spectra derived from https://omlc.org and [13]; last accessed 12/01/2022. Molecular structure of ICG derived from http://molview.org on 12/01/2022.

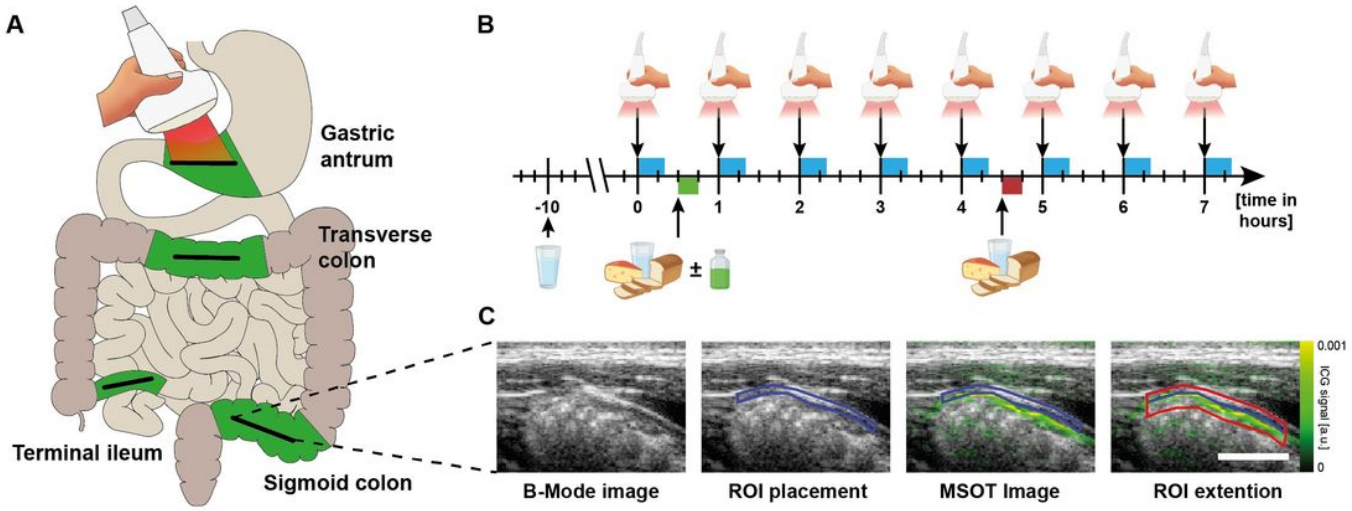

Figure 2

Study flow and MSOT data processing

A: Four intestinal segments (gastric antrum, terminal ileum, transverse colon, and sigmoid colon) were images by handheld MSOT.

B: MSOT imaging was performed on eight imaging timepoints on two separate days. On both days subjects received two standardized meals 30 minutes after the first and fourth imaging timepoint. On the

second day 50mg of ICG in 150ml water was ingested by every subject immediately before the second imaging timepoint.

C: Co-registered B-mode images were used for anatomical guidance an region of interest (ROI) placement. Thereafter, semi-automated ROI extention was applied to outline the area of potential ICG signal detection. White bar represent 1cm.

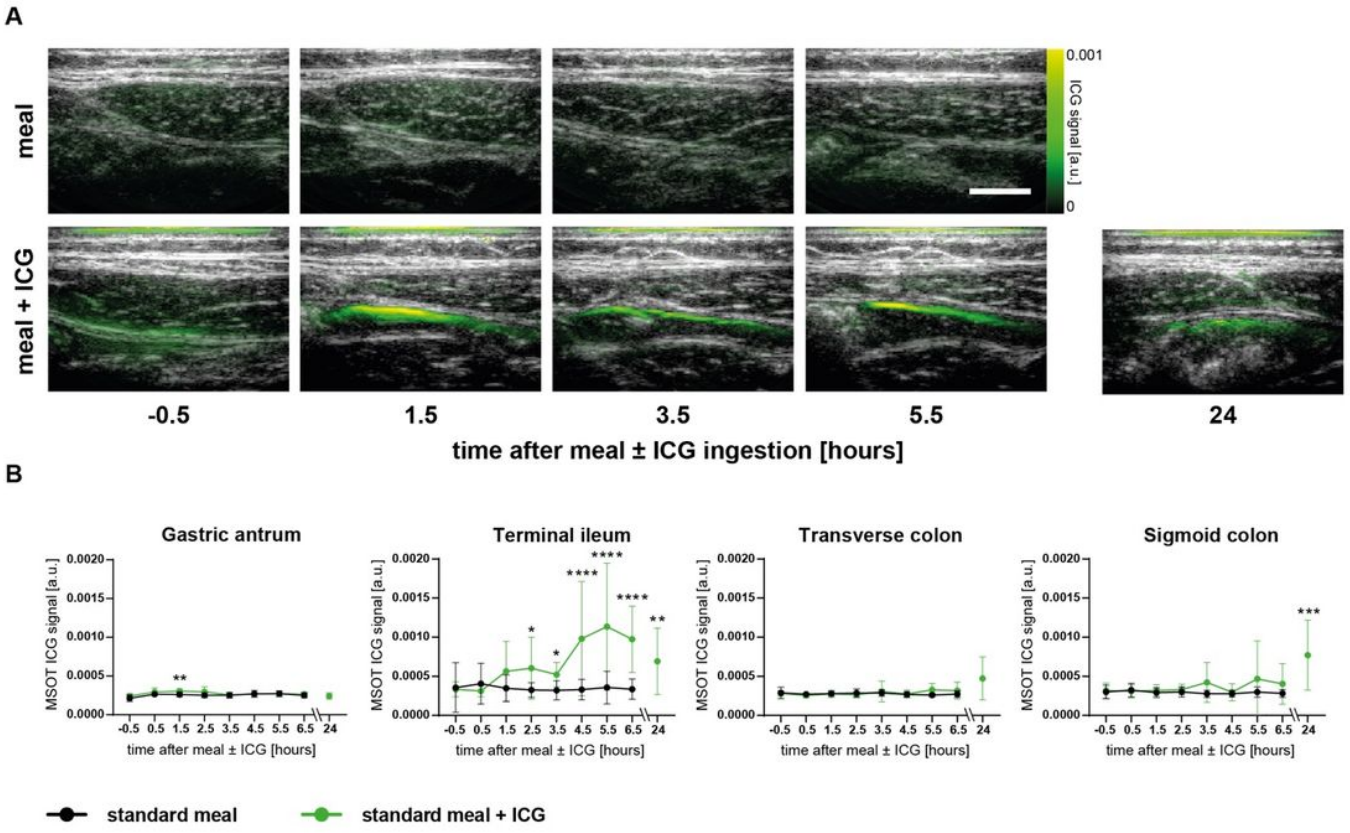

Figure 3

Contrast-enhanced MSOT for the assessment of gastrointestinal transit

A: MSOT ICG signals were detected from 1.5 hours after oral ICG intake in the terminal ileum. In contrast, no ICG signals were detected in the control study arm. White bars represent 1cm.

B: MSOT ICG signal quantification of each imaging timepoint of the day with and without ICG ingestion in the gastric antrum, terminal ileum, transverse colon, and sigmoid colon. Dots and whiskers represent mean and SD. Asterisks represent significant differences. * P<0.05 ** P<0.01 *** P<0.001 **** P<0.0001.

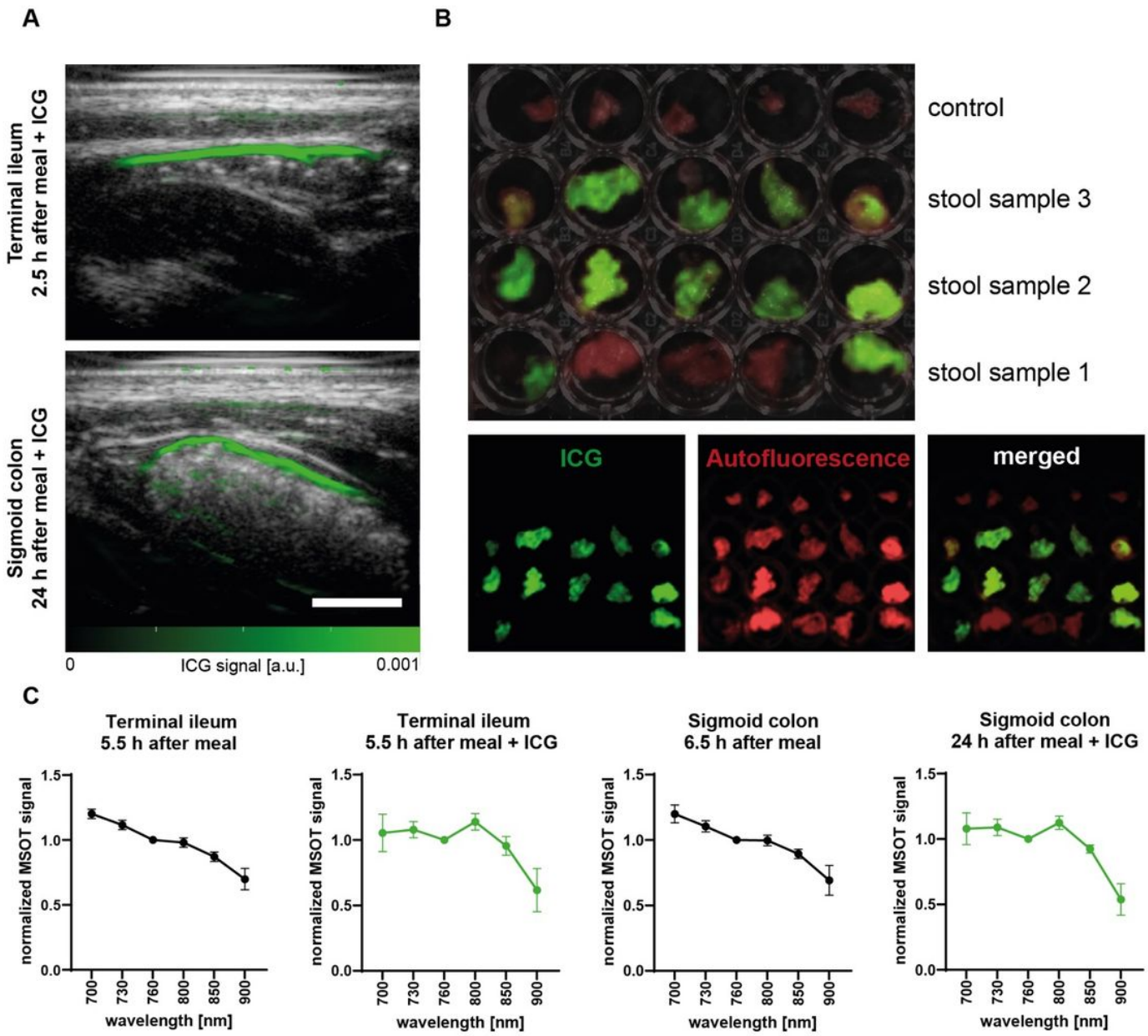

Figure 4

Confirmation of MSOT ICG signals in the stool

A: MSOT ICG signals were detected timely after oral ICG intake in the terminal ileum and with expected delay on the next day in the sigmoid colon. White bars represent 1cm.

B: From n=5 subjectes three conescutive stool samples after oral ICG intake were analysed by flourescent imaging. Factory presets for ICG fluorescence and tissue autofluorescence signals were used.

C: Optoacoustic spectra 5.5 hours after ICG intake in the terminal ileum and 24 hours after ICG intake in the sigmoid colon compared with corresponding timepoints of the day without ICG intake. Dots and

whiskers represent mean and SD.

Supplementary Files

This is a list of supplementary files associated with this preprint. Click to download.

- SupplementaryVideo1.mp4
- SupplementaryVideo2.mp4
- SupplementtoMSOTICGFINAL2.docx